

Full Length Research Paper

Investigation on end anchoring of CFRP strengthened steel I-beams

Kambiz Narmashiri^{1,2*}, Mohd Zamin Jumaat¹ and N. H. Ramli Sulong¹

¹Civil Engineering Department, Faculty of Engineering, University of Malaya, Kuala Lumpur 50603, Malaysia.

²Civil Engineering Department, Faculty of Engineering, Islamic Azad University, Zahedan 98168, Iran.

Accepted 20 August, 2010

Problems that frequently occur in carbon fibre reinforced polymer (CFRP) flexural strengthened steel structures include the peeling and debonding at the tip of the CFRP plate. This paper presents a study on the effectiveness of using steel plates and bolts as end-anchors to address these problems. Four steel I-beams were tested to failure. The first specimen was not strengthened and was used as the control beam. The second beam was strengthened with a CFRP plate without any end-anchoring. The third and fourth specimens were strengthened and end-anchored using steel plates and bolts. The number of bolts was the same, however, the length of the steel anchor plates was varied. The beams were tested under four point loads and loaded incrementally while the deflection and strain readings on the critical parts of the beams were recorded. For the numerical study, full three dimensional (3D) simulation and nonlinear static analysis was carried out using ANSYS software. The results indicate that the anchored beams had higher load capacities of up to 24% compared to the non-strengthened beam. End-anchoring with closer bolt spacing was more effective. Both experimental and numerical results are in good agreement highlighting the accuracy of the developed numerical model.

Key words: End anchoring, carbon fibre reinforced polymer (CFRP), I-beam, steel, strengthening.

INTRODUCTION

Structures may need to be strengthened because of a design fault, construction error, or change in function. Various methods are used to strengthen different structures. For steel structures, these include applying additional steel parts or fibre reinforced polymer (FRP), external prestressing, and bridging the gap between the supports.

Nowadays, the most commonly used material for strengthening steel structures is FRP. However, flexural strengthening steel beam by using FRP usually suffers serious problems in the form of peeling and debonding at the end of the FRP plate. This is normally attributed to the very high stress and strain intensity that occurs at the end of the plates (Sen et al., 2001; Deng et al., 2004; Buyukozturk et al., 2004; Al-Emrani et al., 2005; Schnrech et al., 2006, 2007; Deng and Lee 2007a, b; Rizkalla et al.,

2008; Kaan, 2008; Linghoff et al., 2009; Haghani et al., 2009; Seleem et al., 2010; Narmashiri and Jumaat, 2010).

Deng et al. (2004) found that high stress concentrations and peeling stress occur at the end of the plates. Al-Emrani et al. (2005) reported that two failure modes occur at the end of the CFRP plates: (a) interlaminar shear failure (delamination) at the end of the laminate, and (b) debonding failure due to maximum shear in the bond line at the end of the laminate.

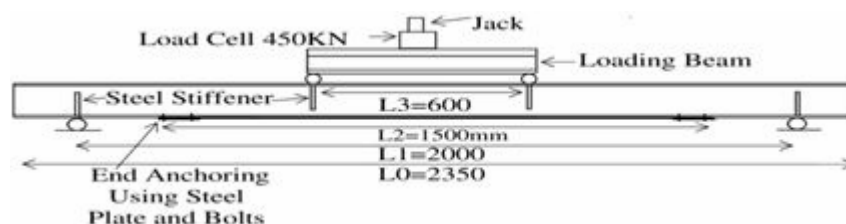
Deng and Lee (2007a, b) demonstrated that debonding occurs as a result of the maximum interfacial stress reaching a critical value, which occurs at the end of the CFRP plate.

Some researchers have demonstrated methods to overcome these problems (peeling and debonding at the end of the CFRP plates) for steel structures by using a tapered CFRP end cutting shape (Deng et al., 2004; Schnrech et al., 2007; Deng and Lee 2007a, b; Rizkalla et al., 2008; Linghoff et al., 2009; Haghani et al., 2009; Seleem et al., 2010). It is difficult to cut the tips of CFRP in a tapered shape, especially for thin CFRP plates.

*Corresponding author. E-mail: kambiz@narmashiri.com, narmashiri@yahoo.com, narmashiri@siswa.um.edu.my. Tel: +60-173585397. Fax: +60-3-79675318.

Table 1. Steel I-beam and steel plate dimensions and properties.

Mild steel A36 (ASTM)														
Steel I-beams dimensions (mm)				Steel plates dimensions (mm)						E-Modulus (N/mm ²)	Stress (N/mm ²)		Strain	
Width	Height	Flange Thick.	Web Thick.	Steel plate A			Steel plate B				Mean value	Yielding (F _y)	Ultimate (F _u)	Yielding (ε _y) %
				Width	Length	Thick.	Width	Length	Thick.					
100	150	10	6.6	150	200	6	150	100	6	200000	250	370	0.12	13.5

**Figure 1.** Test setup.

Although this approach decreased the peeling stress, it did not prevent peeling and debonding completely.

It seems that anchoring the end of CFRP plates decreases the effects of peeling and debonding at the end of CFRP plates for both steel and concrete structures. Normally, U or L shapes are used for FRP end-anchoring for concrete structures (Jumaat and Alam, 2008), however, these shapes are impractical for steel I-beams because of their geometric shapes.

Using a CFRP overlay in strengthened steel structures can help to retard peeling and debonding at the end of the plates considerably (Kaan, 2008), however, special mechanical equipment is required to make CFRP overlays.

The application of steel plates and bolts for CFRP end-anchoring has been recently introduced. Motavalli and Czaderski (2007) demonstrated seismic retrofitting of a masonry

shear wall by using GFRP fabric and additional CFRP plates that were anchored in the concrete using end-anchor plates.

The strengthening of reinforced concrete slabs with mechanically-anchored unbonded FRP system by using steel plates and bolts was researched by Maddawy and Soudki (2008). The anchor system that they used consisted of a steel plate with four bolts. The steel plate was placed below the CFRP plate and held in place using bolts that were inserted into holes that were pre-drilled through the slab thickness at desired locations.

This kind of anchoring damaged the slab, and changed the failure modes due to the holes in the slab.

Applying a three-piece clamping system at the end of the CFRP plates for steel-concrete composite bridges increased the resistance against peeling and debonding (Sen et al., 2001),

however, using this clamping system did not increase the load capacity in the whole beam because the failure mode was governed by the holes in the CFRP plates.

The objectives of this research are as follows: (a) to study the effectiveness of end-anchoring for steel I-beams by using steel plates and bolts; (b) to investigate the effects of the bolt arrangement in the anchor plates, and (c) to study the structural behaviour of CFRP end-anchored beams by using steel plates.

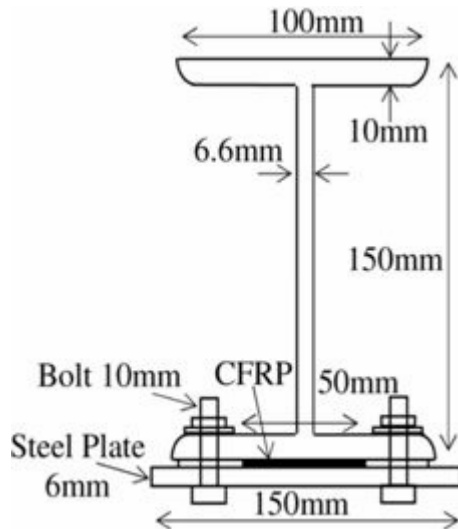
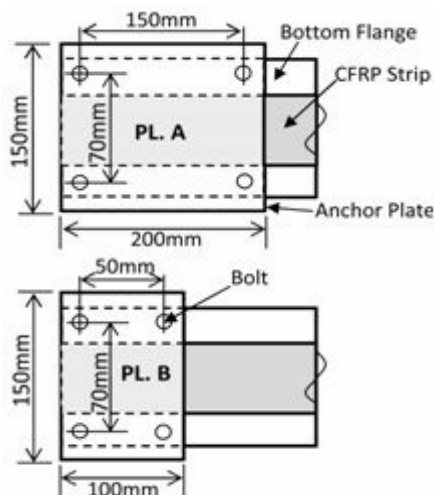
MATERIALS AND METHODS

Steel beam

In this research, steel I-sections from grade A36 (ASTM) were strengthened by using CFRP plates. Table 1 shows the dimensions and material properties of the beams, and Figure 1 indicates the schematic of the specimens.

Table 2. Bolt dimensions and properties.

Diameter (mm)	Stress (N/ mm ²)	
Nominal	Yielding (F _y)	Ultimate (F _u)
10	585	825

**Figure 2.** Cross sectional of steel I-beam.**Figure 3.** Dimensions of the steel plates.

Steel anchor plate

To anchor the end of the CFRP plates, two different steel plate sizes were used. Each plate had four holes, which were connected to the bottom flange of the steel beam at the end of the CFRP plate. Although the width and thickness of the plates were the same, their lengths were varied to account for different bolt spacing. The dimensions of the steel anchor plates are given in Table 1. The material properties of the anchor plates were the same as the steel I-beams, as shown in Table 1. In addition, the specifications of the anchor plates are illustrated in Figures 2 and 3.

Bolt

To increase the bonding between the anchor plates, adhesive, CFRP, and steel beam, the steel anchor plates were connected to the bottom flange by four bolts at each CFRP tip (Figure 2). The specifications and material properties of the bolts are shown in Table 2.

CFRP plate

Carbon fibre reinforced polymer has been widely utilised to strengthen structural elements. As CFRP has high tensile strength, it has been installed on the tensile region to improve the load bearing capacity of structures. For steel I-beams the best region for installing CFRP is the outer side of the tensile (bottom) flange. The dimensions and properties of the chosen CFRP plates are shown in Table 3 (SIKA Product Information, 2008).

Adhesive

The CFRP plates were installed on the beam flange by using special epoxy. The epoxy must be strong to bear the high stress generated during loading (Schnrech et al., 2005, 2006). Nowadays, producing high strength epoxy is possible due to modern technology. The specification and material properties of the chosen adhesive are shown in Table 4 (SIKA Product Information, 2008).

Specimens

To investigate the effects of CFRP end-anchoring, four specimens were tested. The specifications of the specimens are shown in Table 5. The schematic of the specimens and test setup are illustrated in Figure 1. Figure 2 illustrates the detailed specifications of the steel section.

Preparation of the specimens

The following processes were carried out for the preparation of the specimens. First, the steel plates and bottom flange of the steel I-beams were punched in the region of the end of CFRP plates. Second, according to the SIKA product instruction (2008), the surfaces were sandblasted based on Swedish Standard SA 2.5. It should be noted that the maximum duration after sandblasting and before gluing CFRP plates at a temperature of +30°C is 48 h.

Then, the CFRP plates were glued to the bottom flange of the specimens. Subsequently, both ends of the CFRP plates were covered by adhesive. The length of the covered region must be the same as the plate's length. Then, the surfaces of the steel anchor plate that were to be pasted at the end of the CFRP plates were covered with adhesive. Subsequently, the steel plates were placed at the end of the CFRP plates. Then, the adhesive that covered the holes for the bolts was cleaned. After one week, the last stage, when the adhesive had hardened appropriately, was tightening the bolts.

Table 3. CFRP plate dimensions and properties.

CFRP plate: Sika® CarboDur® S512/80												
Dimensions (mm)			E-modulus (N/ mm ²)				Tensile strength (N/ mm ²)				Strain	
Width	Thick.	Length	Mean value	Min. value	5% fracture value	95% fracture value	Mean value	Min. value	5% fracture value	95% fracture value	Strain at break	Design strain
50	1.2	1500	165000	> 160000	162000	180000	3100	> 2800	3000	3600	> 1.7%	< 0.85%

Table 4. Adhesive dimensions and properties.

Adhesive: Sikadur® -30										
Dimensions (mm)			Compressive strength (N/ mm ²)		Tensile strength (N/ mm ²)		Shear strength (N/ mm ²)		Bond strength on steel	
Width	Thick.	Length	E-Modulus	Strength 7 days	E-Modulus	Strength 7 days	Strength 7 days	Strength 7 days	Mean value	Min. value
50	1.0	1500	9600	70 - 95	11200	24 - 31	14 - 19	30	> 21	

Table 5. Specifications and load capacities of the specimens.

Specimen	CFRP plate length (mm)	CFRP end-anchor plate	Load capacity			
			Load (kN) from experimental tests	Load increment compared to B1 (%)	Load increment compared to B2 (%)	Load (kN) from numerical analysis
B1	0	N/A	181.69	0	-	170.93
B2	1500	N/A	206.24	13.51	0	191.13
B3	1500	Plate A	216.15	18.97	4.81	201.48
B4	1500	Plate B	225.6	24.17	9.39	211.22

Test setup

The experimental setup is based on the four point bending test (Narmashiri et al., 2010). In order to measure strain and deflection, strain gauges and linear variable deformation transducer (LVDT) were installed in different regions of the specimens. Figure 4 shows the locations and directions of strain gauges. As shown, one strain gauge was installed on the CFRP plate at the mid-span in

the longitudinal direction to measure the tensile strain on the CFRP. In addition, strain gauges were installed along the length of the CFRP plate to measure the strain along the whole length of the plate. Another strain gauge was installed on the inner side of the beam's bottom flange to measure normal tensile strain on the steel at the mid-span. One LVDT was installed horizontally at the mid-span on the web to measure the lateral deflection, and another LVDT was installed vertically at the mid-span on the

beam's bottom flange to measure the vertical deflection. The load was applied by using a hydraulic jack via a load cell of 450 kN capacity. The load was transferred from the jack to the main specimen by using a loading beam. The middle of the loading beam was subjected to jack pressure, and two symmetrical point loads were applied to transfer the load's pressure to the main specimen. Two roller supports carried the reactions, therefore, the loading state was four incremental bending points loads.

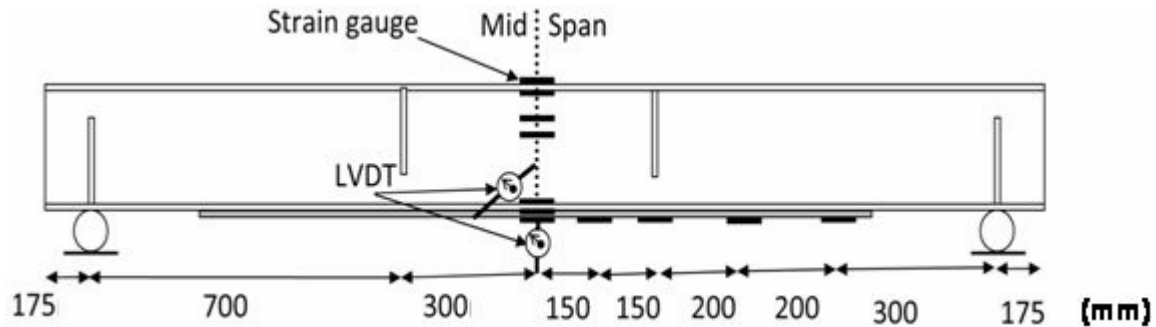


Figure 4. Locations of strain gauges.

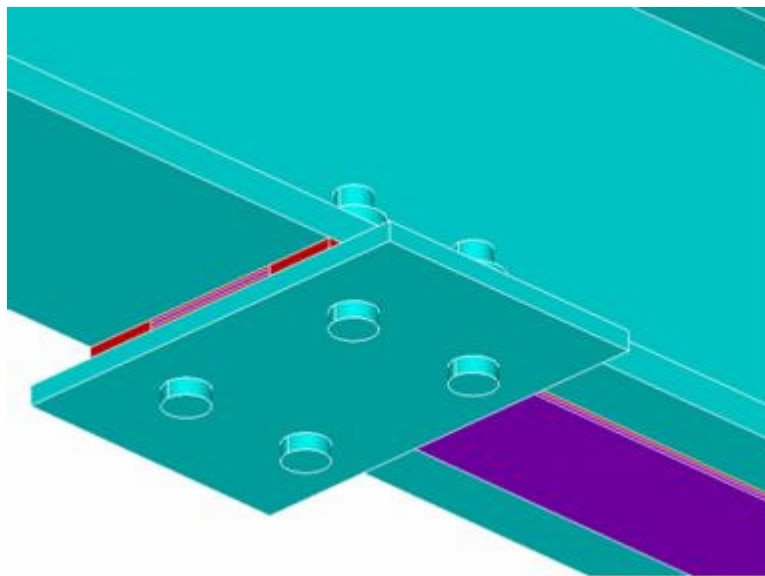


Figure 5. View of end-anchor plate, obtained from ANSYS.

Numerical simulation

To evaluate the experimental test, full three-dimensional (3D) simulation using ANSYS software was performed. The steel I-sections, steel stiffeners, steel anchor plates, steel bolts, CFRP plates, and adhesive were simulated by using 3D solid triangle elements (Ten nodes 187).

The interface of common surfaces was defined between the steel I-beam, adhesive, CFRP plates, bolts, and steel anchor plate (Narmashiri et al., 2010). Debonding and peeling occurred when the plastic strain exceeded the ultimate strain. Non-linear static analysis was carried out to achieve debonding and peeling.

In this case, the load was applied incrementally until the plastic strain in the first element reached the ultimate strain. The linear and nonlinear properties of the materials were defined. The material properties of the CFRP plate were defined as linear and orthotropic because CFRP materials have linear properties that are unidirectional. The steel beams, plates, bolts, and adhesive were defined as non-linear properties.

Figures 5 and 6 shows the simulated models of the end-anchoring, and the meshed specimen, respectively. To mesh the elements, a combination of the auto meshing and map meshing

were used. In critical regions, such as the location of the anchor plate, the elements were meshed smaller than the other regions. To validate the experimental test with the simulation method, the tensile strain on the CFRP plate at the mid-span for specimen B2 is chosen as a sample. The numerical and experimental outputs were compared, as shown in Figure 7. In this figure, the vertical axis is the load in kN, and the horizontal axis is the tensile strain on CFRP in Microns. The graph represents the high level of conformity between the numerical and experimental results. The comparison between the results of the experimental and numerical studies on the other parameters, such as strain and deflection on different regions, also shows a good agreement (Narmashiri and Jumaat, 2010). However, these are not presented here because of the length of the paper.

RESULTS AND DISCUSSIONS

Load capacity

Normally, one of the most important parameters required



Figure 6. Meshing of end-anchor plate, obtained from ANSYS.

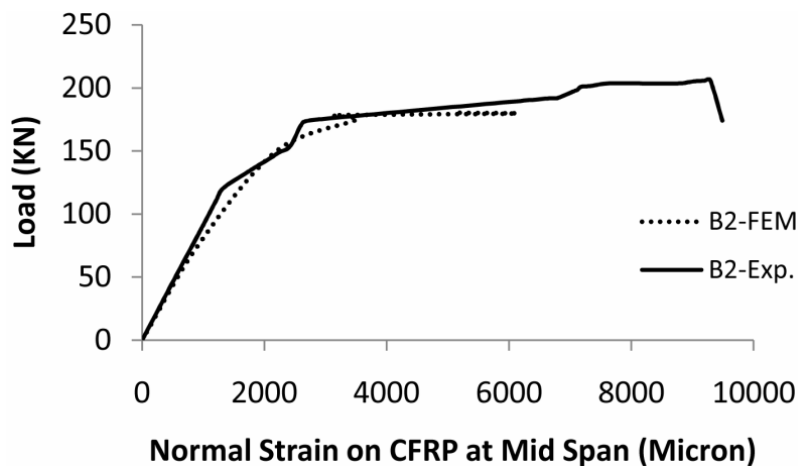


Figure 7. Validation of the experimental results with numerical simulation.

in the strengthening of structures is the increment of the load capacity of the upgraded specimens compared to the non strengthened specimens.

Table 5 shows the load capacity for different specimens. It shows that by using end-anchoring, the load capacity of the steel I-beams improved up to 24%. This means that using anchoring system bonding between the CFRP and the steel resulted in an improvement of the load capacity appropriately.

According to this table, the maximum load increment was obtained by the anchored specimen (B4). This means, that by using a smaller anchor plate (Plate B) the load capacity increased appropriately. However, if the same number of bolts was used for both plates, then the spacing between the bolts in the smaller plate B was less than in the bigger anchor plate A. Using shorter distances

between the bolts created a more rigid zone that helped to increase the bonding at the end of the CFRP plates. Finally, applying shorter bolt spacing caused a significant improvement in the load capacity.

Failure mode shapes

The failure modes of the CFRP before and after anchoring were not the same. Four failure modes are recognized for CFRP flexural strengthened steel-concrete composite beams without anchoring (Al-Emrani et al., 2005): (a) rupture of the laminate at the mid-span when the maximum axial stress in the laminate reaches its ultimate strength; (b) debonding failure due to maximum shear in the bond line at the end of the laminate; (c)



Figure 8. CFRP end delaminating (peeling).



Figure 9. CFRP mid delaminating (splitting).

debonding failure due to maximum shear in the bond line in the middle of the laminate, and (d) interlaminar shear failure (delamination) at the end of the laminate (Figure 8). In this research, steel I-beams without lateral prevention were tested, therefore, the above mentioned failures and one more failure mode were observed: (e) mid-splitting of the CFRP plates below the point loads (Figure 9).

This began from the mid-span and developed along the whole length of the plate. This failure mode occurred due to the asymmetrical stress intensity below the point loads (Figure 10). This stress intensity resulted because of the combination of the overall lateral-torsional-buckling and local buckling. As mentioned, in this study, lateral deformation of the specimens was not prevented, therefore, the beams deformed in both vertical and horizontal directions. This kind of stress distribution was symmetrical in the longitudinal direction, however, it was asymmetrical in

the transverse direction (perpendicular to the beam's axis). This caused the CFRP mid-splitting (failure mode "e").

By using steel plates and bolts as CFRP end-anchoring, the CFRP failure modes were changed as follows: (a) mid-debonding; (b) mid-splitting, and (c) CFRP pulling out (Figure 11). The CFRP end-anchoring was more effective on the delaminating (peeling) and debonding at the end of the plate because the ends of the CFRP plates were covered using the steel anchor plates appropriately. For the anchored specimens, debonding occurred along the whole length of the CFRP plate, except the part of the plates that were covered by the anchor plate. Pulling out of the CFRP plates below the anchor plate occurred when the full capacity of the CFRP was used to support the load. The pulling-out means that the CFRP plates still bear the load after mid-debonding.

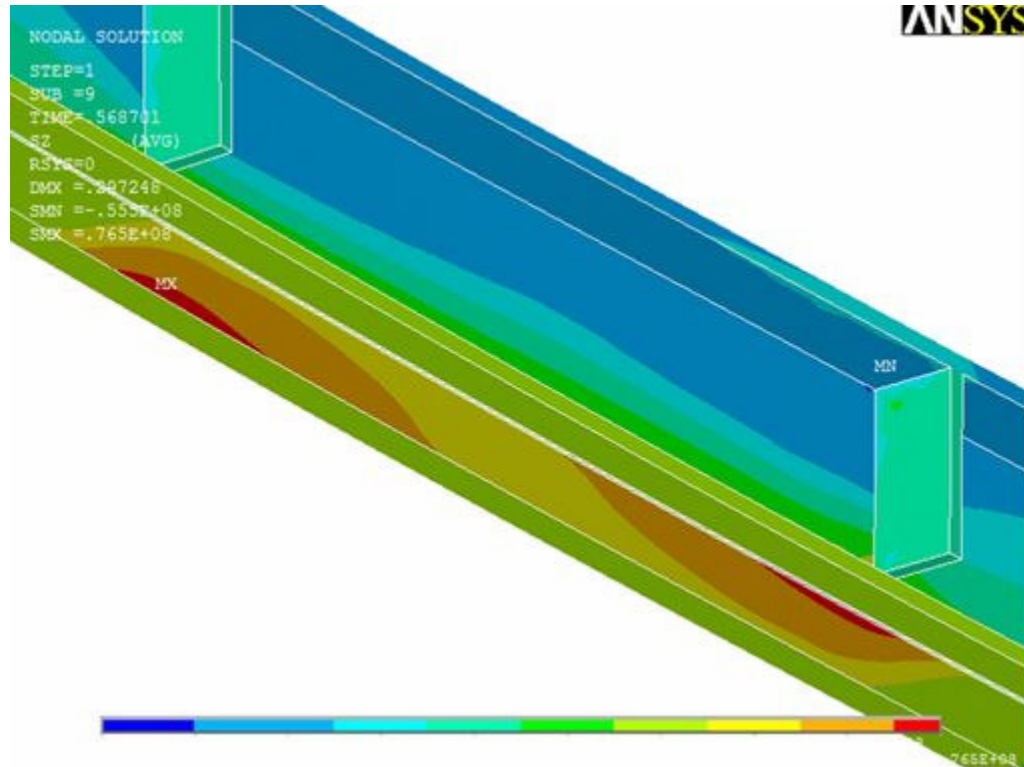


Figure 10. Tensile stress intensity on the CFRP.



Figure 11. CFRP pulling out.

Strain on the CFRP plate

As mentioned above, end-anchoring changed the failure of the CFRP plates and improved the load capacity. Here, the effects of anchoring on the strain of the CFRP plate was investigated.

To investigate the effect of CFRP end-anchoring on the CFRP plate, the tensile strain at the mid-span was chosen. Figure 12 shows the tensile strain on CFRP at the mid-span versus load. This shows that by using anchor plates (B3, B4), the strain on the CFRP

decreased appreciably compared to the non-anchored specimen (B2), particularly in the plastic region.

To investigate the effects of the anchoring system on the strain along the length of the plate, strain gauges were installed on the CFRP plate (Figure 4). Figure 13 shows the distribution of the strain on CFRP plates for different specimens at the load level of 180kN (after yielding). This shows that the application of the anchoring system reduced the strain appreciably throughout the whole length of the plate, especially below the point loads and at the mid-span.

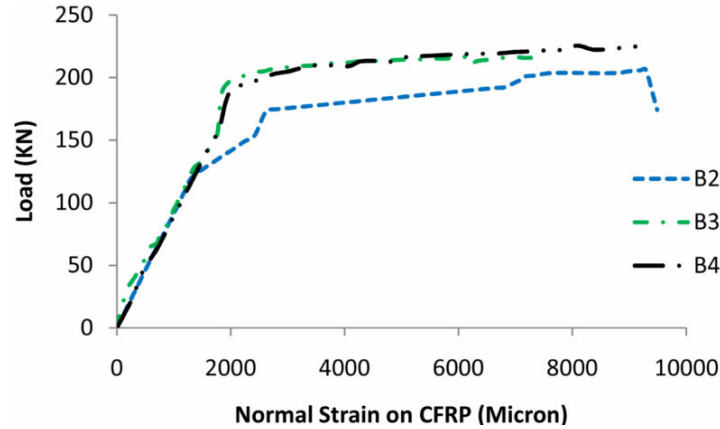


Figure 12. Tensile strain on CFRP plates at the mid-span.

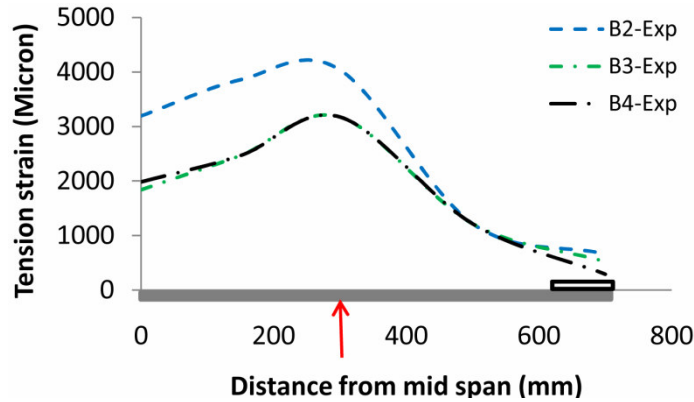


Figure 13. Tensile strain along the length of CFRP plates for load level of 180 kN.

It can be concluded that end-anchoring not only influenced the ends of the CFRP plates, but that it also reduced the strain along the whole length of the plate appropriately.

Lateral-torsional-buckling

One of the behaviours of an unrestrained steel I-beam is lateral-torsional-buckling. Here, the effects of applying steel anchor plates and bolts on the lateral-torsional-buckling in light of lateral deflection at the mid-span are investigated.

Figure 14 shows a deformed specimen based on experimental results. It shows that the top flange had more lateral deformation than the bottom flange because the top flange located in the compression region and buckled in both horizontal and vertical directions.

As Figure 14 demonstrates, the lateral deflection was not exactly symmetrical. This asymmetrical behaviour was observed in both the experimental and numerical studies. The asymmetrical behaviour occurred, especially



Figure 14. Lateral deformation (experiment).

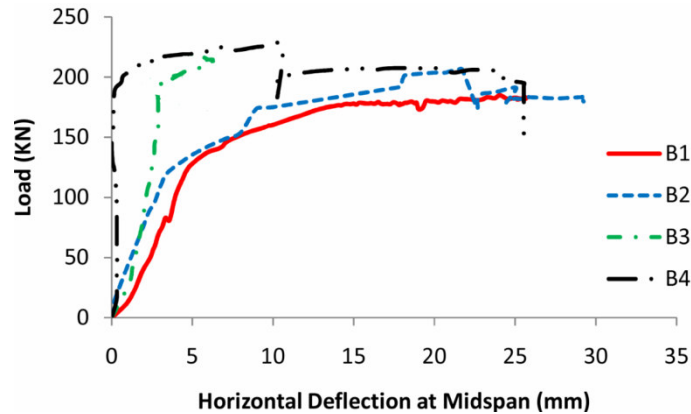


Figure 15. Horizontal deflection at the mid-span.

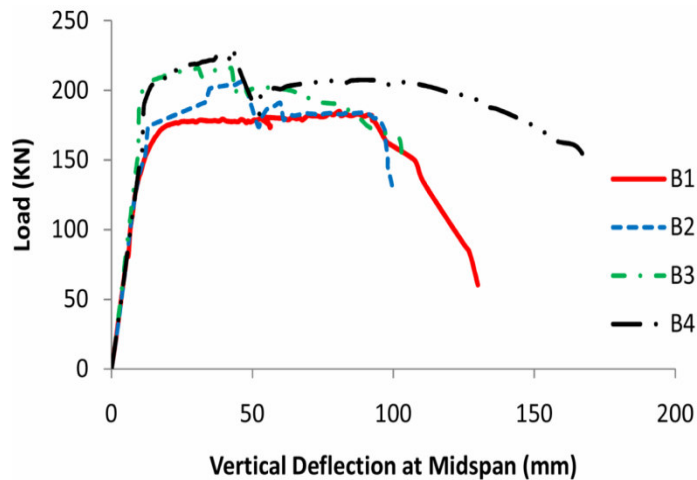


Figure 16. Vertical deflection at the mid-span.

after yielding. In the experimental test, load eccentricity, imperfection, and non-homogenous material properties may influence this asymmetrical behaviour. In the simulation modelling, the asymmetrical meshing of elements that automatically generated by the software caused asymmetrical behaviour.

To measure the lateral deflection, a LVDT was installed horizontally on the web at the mid-span (Figure 4). Figure 15 indicates the variation of lateral deflection versus load. It shows that the lateral deflection of the strengthened specimen (B2) was less than the non-strengthened beam (B1). A reduction in both the elastic and plastic region was observed. In addition, it shows that the anchored specimens experienced less lateral deflection compared to the non-anchored beam (B2). Moreover, specimen B4 had less lateral deflection than specimen B3.

Finally, it can be concluded that by applying steel plates and bolts, the lateral deflection decreased notably. By using shorter bolt spacing, the stability of the beam in out of plane improved appropriately.

Vertical deflection

One of the most important parameters in the flexural strengthening of structures is the decrement of the vertical deflection for the strengthened specimen compared to the non-strengthened specimen. Furthermore, the reduction of the vertical deflection of the strengthened specimen shows the amount of flexural stiffness after strengthening.

Figure 16 illustrates that in the elastic region, there were no differences in the deflections of the strengthened specimen (B2) and the non-strengthened beam (B1). However, in the plastic region, the deflection of specimen B2 was less than specimen B1. In addition, this figure demonstrates that the application of steel anchor plates (B3, B4) decreased the vertical deformation considerably. Overall, in the plastic region the best result achieved by specimen B4. Furthermore, vertical deflection affected by the dimension of the anchor plates (bolt spacing), and the application of a smaller plate (bolt spacing) caused less

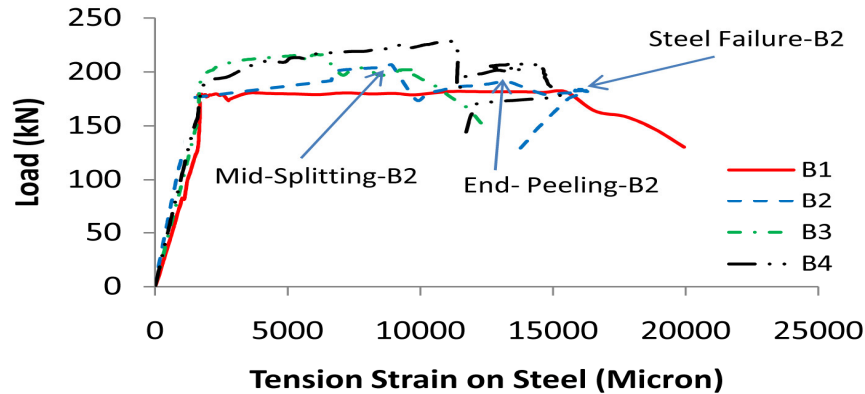


Figure 17. Tensile strain on beam bottom flange at the mid-span.

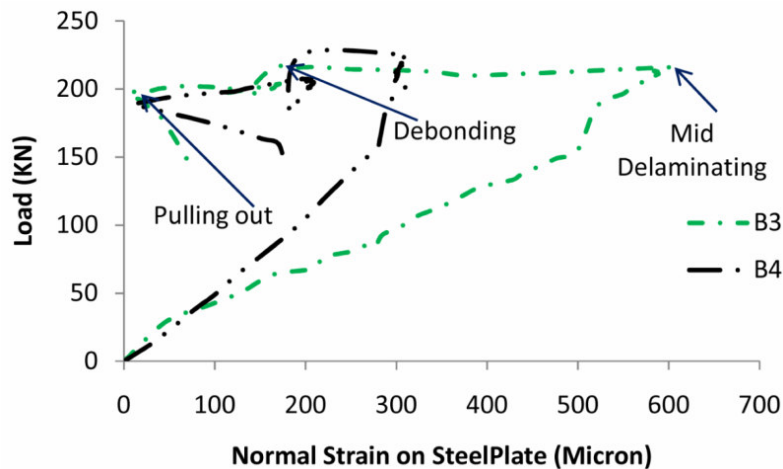


Figure 18. Tensile strain on the steel anchor plates.

vertical deflection. Finally, by applying anchor plates, the vertical deflection of the steel I-beams decreased appreciably, especially in the plastic region.

Strain on the bottom flange

Figure 17 illustrates the variation of the tensile strain on the bottom flange versus the load at the mid-span. This figure shows the effects of both failures of CFRP (mid-splitting and debonding) on the strain, which caused a reduction in the strength of the strengthened beam (B2). In addition, this figure demonstrates that by applying a shorter anchor plate, the bonding of the CFRP increased notably. This behaviour was proven by specimen B4 where the failure only occurred in a single stage. In addition, the behaviour of specimen B4 in decreasing the normal tensile strain was much better than B3 because of the shorter bolt spacing.

Finally, the splitting and debonding caused a reduction in the strength. The application of shorter bolt spacing

further reduced the strain on the steel bottom flange.

Strain on the steel anchor plate

The amount of the interfacial transferred force between the adhesive and anchor plate seems to be related to the steel plate dimension, which is measurable by installing a strain gauge on the steel anchor plate.

Figure 18 illustrates the variation of strain on the anchor plates versus load. The CFRP failure modes of the anchored beams were observed in this figure, that is, mid-delaminating, mid-debonding, and end-pulling out. After delaminating, the strain on the steel plates decreased critically. Then, debonding caused a reduction in the strain on the anchor plates. Thereafter, the pulling out of the CFRP from the bottom of the steel plate caused a significant drop in the strain of the steel plate.

This figure demonstrates that although more strain occurred on the bigger plate (A), which means a greater interfacial force was transferred between the adhesive

and the anchor plate. It did not create more load capacity because there was not enough rigidity compared to the smaller plate.

Conclusions

This study shows that the application of steel plates and bolts is a successful method for CFRP end-anchoring of steel I-beams.

For anchoring steel I-beams, the bolt spacing were more effective than the length of the anchor plates, and using smaller bolt spacing improved the load capacity of the steel I-beams by approximately 24%.

The CFRP failure modes for the non-anchored and anchored steel I-beams were not the same. For the non-anchored beam, the failure modes were: Mid-splitting, mid-debonding, end-peeling, and end-debonding. For the anchored specimens the failure modes were as follows: Mid-splitting, mid-debonding, and end-pulling out. End-anchoring decreased the effects of end-peeling and debonding appropriately.

CFRP end-anchoring decreased the strain and deformation of the whole beam including the tensile strain on CFRP plates, lateral-torsional-buckling (lateral deformation), and vertical deflection considerably. The effects of the end-anchoring were almost significant in the plastic region.

ACKNOWLEDGEMENT

It is gratefully acknowledged that the study presented here was financially supported by the University of Malaya.

REFERENCES

- Al-Emrani M, Linghoff D, Kliger R (2005). Bonding strength and fracture mechanisms in composite steel-CFRP elements. International Symposium on Bond Behaviour of FRP in Structures (BBFS 2005), International Institute for FRP in Construction.
- Buyukozturk O, Gunes O, Karaca E (2004). Progress on understanding debonding problems in reinforced concrete and steel members strengthened using FRP composites. *Constr. Build. Mater.*, 18: 9-19.
- Deng J, Lee MMK (2007a). Behaviour under static loading of metallic beams reinforced with a bonded CFRP plate. *Compos. Struct.*, 78: 232-242.
- Deng J, Lee MMK (2007b). Fatigue performance of metallic beam strengthened with a bonded CFRP plate. *Compos. Struct.*, 78: 222-231.
- Deng J, Lee MMK, Moy SSJ (2004). Stress analysis of steel beams reinforced with a bonded CFRP plate. *Compos. Struct.*, 65: 205-215.
- Haghani R, Al-Emrani M, Kliger R (2009). Interfacial stress analysis of geometrically modified adhesive joints in steel beams strengthened with FRP laminates. *Constr. Build. Mater.*, 23: 1413-1422.
- Jumaat MZ, Alam MA (2008). Behaviour of U and L shaped end anchored steel plate strengthened reinforced concrete beams. *Europn. J. Scient. Res.*, 22: 184-196.
- Kaan BN (2008). Fatigue enhancement of category E' details in steel bridge girders using CFRP materials. Graduate Faculty, University of Kansas, Master of Science, Kansas.
- Linghoff D, Haghani R, Al-emrani M (2009). Carbon-fibre composites for strengthening steel structures. *Thin Wall. Struct.* 47: 1048-1058.
- Maddawy TE, Soudki K (2008). Strengthening of reinforced concrete slabs with mechanically-anchored unbonded FRP system. *Constr. Build. Mater.*, 22: 444-455.
- Motavalli M, Czaderski C (2007). FRP composites for retrofitting of existing Civil Structures in Europe: state-of-the-art review. International Conference of Composites & Polycon., American Composites Manufacturers Association. Tampa, FL, USA.
- Narmashiri K, Zamin Jumaat M, Ramli Sulong NH (2010). Shear strengthening of steel I-beams by using CFRP strips. *Sci. Res. Essays*, 5(16).
- Narmashiri K, Jumaat MZ (2010). Reinforced steel I-beams: A comparison between 2D and 3D simulation. *Simul. Model. Pract. Theory.* (doi:10.1016/j.simpat.2010.08.012)
- Rizkalla S, Dawood M, Schnerch D (2008). Development of a carbon fiber reinforced polymer system for strengthening steel structures. *Compos. Part A-Appl.*, 39: 388-397.
- Schnerch D, Dawood M, Rizkalla S, Sumner E (2007). Proposed design guidelines for strengthening of steel bridges with FRP materials. *Constr. Build. Mater.*, 21: 1001-1010.
- Schnerch D, Dawood M, Sumner E, Rizkalla S (2006). Design guidelines for strengthening of steel-concrete composite beams with high modulus CFRP materials. 7th. International Conference on Short and Medium Span Bridges.
- Schnerch D, Stanford K, Sumner E, Rizkalla S (2005). Bond behavior of CFRP strengthened steel bridges and structures. International Symposium on Bond Behaviour of FRP in Structures (BBFS 2005), International Institute for FRP in Construction.
- Seleem MH, Sharaky IA, Sallam HEM (2010). Flexural behavior of steel beams strengthened by carbon fiber reinforced polymer plates—Three dimensional finite element simulation. *Mater. Des.*, 31: 1317–1324.
- Sen R, Liby L, Mullins G (2001). Strengthening steel bridge section using CFRP laminates. *Compos. Part B-Eng.*, 32: 309-322.
- SIKA Product Information (2008). Second ed., Sika@ Kimia Sdn Bhd., Kuala Lumpur.